Published in final edited form as:
Dev Dyn. 2014 May ; 243(5): 629–639. doi:10.1002/dvdy.24104.

Tbx4 Interacts With the Short Stature Homeobox Gene *Shox2* in Limb Development

Anne Glaser[1], **Ripla Arora**[2], **Sandra Hoffmann**[1], **Li Li**[3], **Norbert Gretz**[3], **Virginia E. Papaioannou**[2], and **Gudrun A. Rappold**[1,*]

[1]Department of Human Molecular Genetics, University of Heidelberg, Heidelberg, Germany

[2]Department of Genetics and Development, Columbia University Medical Center, New York, New York

[3]Medical Research Center, University of Heidelberg, Mannheim, Germany

Abstract

Background—The short stature homeodomain transcription factors SHOX and SHOX2 play key roles in limb formation. To gain more insight into genes regulated by Shox2 during limb development, we analyzed expression profiles of WT and *Shox2*$^{-/-}$ mouse embryonic limbs and identified the T-Box transcription factor Tbx4 as a potential downstream target. Tbx4 is known to exert essential functions in skeletal and muscular hindlimb development. In humans, haploinsufficiency of *TBX4* causes small patella syndrome, a skeletal dysplasia characterized by anomalies of the knee, pelvis, and foot.

Results—Here, we demonstrate an inhibitory regulatory effect of Shox2 on *Tbx4* specifically in the forelimbs. We also show that Tbx4 activates *Shox2* expression in fore- and hindlimbs, suggesting Shox2 as a feedback modulator of Tbx4. Using EMSA studies, we find that Tbx4/TBX4 is able to bind to distinct T-box binding sites within the mouse and human *Shox2/SHOX2* promoter.

Conclusions—Our data identifies Tbx4 as a novel transcriptional activator of *Shox2* during murine fore- and hindlimb development. *Tbx4* is also regulated by Shox2 specifically in the forelimb bud possibly via a feedback mechanism. These data extend our understanding of the role and regulation of Tbx4 and Shox2 in limb development and limb associated diseases.

Introduction

Vertebrate limb buds initially consist of proliferating mesenchymal cells enveloped by ectoderm that emerge from the lateral plate mesoderm (LPM). As outgrowth continues, progenitor cells from the LPM differentiate into bones, tendons, and some of the vasculature whereas muscles are formed by migrating precursors derived from adjacent somites (Pearse

*Correspondence to: Gudrun A. Rappold; Institute of Human Genetics; Department of Human Molecular Genetics, INF 366, 69120 Heidelberg, Germany. Gudrun.Rappold@med.uni-heidelberg.de.

Additional Supporting Information may be found in the online version of this article.

The authors declare there was no conflict of interest.

et al., 2007). Skeletal elements are formed by mesenchymal condensations, which differentiate into chondrocytes and are later replaced by bone (Kronenberg, 2003). The correct patterning of the developing limbs requires a coordinated network of signaling molecules interlinked by feedback loops and their targets. The proximodistal outgrowth and patterning is controlled by the apical ectodermal ridge (AER) via a positive FGF feedback loop resulting in the formation of stylopod, zeugopod, and autopod (Mariani and Martin, 2003; Zeller et al., 2009; Duboc and Logan, 2011).

Transcriptional regulatory genes orchestrate the expression of numerous target genes important for limb patterning (Mariani and Martin, 2003). Various defects in limb formation arise from mutations in these genes and genes of the Hox and T-box transcription factor families provide prominent examples. Simultaneous mutations of *Hoxa11/Hoxd11* in mice, e.g., lead to a severe shortening of the ulna and radius and *Hoxa10/Hoxc10/Hoxd10*-deficient mice develop shortened femurs (Davis et al., 1995; Wellik and Capecchi, 2003; Boulet and Capecchi, 2004). Mutations in T-box transcription factor genes lead to various human syndromes associated with limb malformations, including small patella syndrome (*TBX4*) and Holt-Oram syndrome (*TBX5*) (Basson et al., 1997; Li et al., 1997; Bongers et al., 2004).

During limb development, *Tbx4* and its paralog *Tbx5* show almost exclusive expression patterns with *Tbx4* mainly expressed in the hindlimb and *Tbx5* expression restricted to the forelimb (Chapman et al., 1996; Gibson-Brown et al., 1996; Naiche et al., 2011). The expression in their respective limb fields suggests that Tbx4 and Tbx5 might have a role in determining limb-type identity (Duboc and Logan, 2011). Tbx5 and Tbx4 also have well-described roles in initiation and initial outgrowth of the fore- and hindlimb buds. Due to an insufficient establishment of the Fgf signaling loop between the LPM and the overlying ectoderm, mice deficient for *Tbx4* or *Tbx5* do not form limb buds properly. *Fgf10* was shown to be a target of both transcription factors, but in contrast to Tbx5, Tbx4 is not required exclusively for *Fgf10* expression (Ng et al., 2002; Agarwal et al., 2003; Naiche and Papaioannou, 2003; Rallis et al., 2003).

The short stature homeobox-containing gene *SHOX* and its paralog *SHOX2* encode two members of paired related homeodomain transcription factors with crucial functions during embryonic development. *SHOX* was identified as a gene controlling human growth as mutations and deletions lead to the short stature and skeletal deformities associated with Leri-Weill dyschondrosteosis (LWD) and Langer mesomelic dysplasia (LMD) (Belin et al., 1998; Shears et al., 1998; Schiller et al., 2000; Zinn et al., 2002; Benito-Sanz et al., 2005). Moreover, *SHOX* defects have been identified in the non-syndromic isolated forms of short stature with a prevalence of 5–17% in geographically different populations (Chen et al., 2009; Rosilio et al., 2012). A characteristic clinical feature of LWD and LMD patients is a mesomelic shortening of the zeugopod elements (the forearms and lower legs) as well as a typical malformation of the forearms, termed Madelung deformity. The role of SHOX in the etiology of short stature suggests crucial functions in proximodistal limb formation and bone development.

A paralog of the *SHOX* gene, *SHOX2*, has an identical homeo-domain (60 amino acids) and shows an overall similarity on the amino acid level of 65% (Blaschke et al., 1998; Semina et al., 1998). Although *SHOX2* has not been linked to any human phenotype so far, analysis of Shox2-deficient mouse models revealed that *Shox2* also plays a key role in limb development, where it controls neural, muscular, and skeletal processes. Both conditional and conventional knockout of *Shox2* lead to a dramatic shortening of the stylopod elements of the limbs due to delayed chondrocyte maturation and differentiation (Cobb et al., 2006; Yu et al., 2007). In addition, loss of Shox2 function causes altered muscular development and innervation defects in the proximal forelimbs (Vickerman et al., 2011). Different genes in limb development including *Runx2/3*, *Ihh*, and *Bmp4* have been shown to be regulated by Shox2 (Cobb et al., 2006; Yu et al., 2007; Vickerman et al., 2011), while *Hoxa11* and *Hoxd11* act upstream of Shox2 to regulate chondrocyte differentiation (Gross et al., 2012).

To further elucidate Shox2-dependent signaling pathways during limb development, we searched for new Shox2 target genes using microarray expression profiling. *Tbx4* was found to be dynamically regulated by Shox2 in the forelimb, but not in the hindlimb, which raised our interest. In addition, Tbx4 was identified as a novel transcriptional activator of *Shox2* in both fore-and hindlimbs, strongly suggesting that Shox2 acts as a feedback modulator of *Tbx4* during limb development.

Results

Tbx4 Expression Is Increased in the Developing Forelimbs of *Shox2*-Deficient Mice

To identify Shox2-regulated genes during limb development, we used our previously generated *Shox2* knockout mouse model (Blaschke et al., 2007), depicting a severe shortening of mutant ($Shox2^{-/-}$) fore- and hindlimbs (Fig. 1) consistent with other *Shox2* knockout mouse models (Cobb et al., 2006; Yu et al., 2007). To uncover novel *Shox2* transcriptional target genes in limbs, gene expression was compared in wildtype (WT) and *Shox2* mutants, first using pooled fore- and hindlimb tissue at stage E12.5 and subsequently forelimb tissue at stage E11.5 by microarray analysis. Among differentially regulated putative candidate genes (see Suppl. Table S1), the well-known transcription factor *Tbx4* was upregulated in the limbs of $Shox2^{-/-}$ embryos at both developmental stages, E11.5 and E12.5. As *Tbx4* has essential functions in skeletal and muscular development of the hindlimbs, similar to *Shox2*, we chose it for further analysis.

As a first step in validating *Tbx4* as a putative target gene of Shox2, we compared the expression of both genes in mouse embryos of different developmental stages by in situ hybridization (Fig. 2). *Shox2* expression starts at the onset of limb outgrowth at E9.5 in the forelimb (Fig. 2A a). During later stages, *Shox2* is broadly expressed in fore- and hindlimbs, at E10.5 throughout the whole limb buds and from E11.5 onwards restricted to the proximal part of the limbs (Fig. 2A b–e). As shown previously (Naiche et al., 2011), *Tbx4* is only transiently expressed in the forelimb, starting at E10.5 in a discrete localized region of the proximal limb bud and decreasing at E11.5 (Fig. 2A g, h). Then, beginning at E11.5, *Tbx4* is expressed more diffusely in the distal part of the forelimb and proceeds distally between E12.5 and E13.5 (Fig. 2A h–j). In the hindlimb field, strong *Tbx4* expression can be observed before hindlimb outgrowth, at E9.5, in the lateral plate mesoderm (LPM) (Fig. 2A

f). Expression continues from E10.5 until E12.5 in the entire hindlimb bud, becoming more distally restricted at E13.5 (Fig. 2A g–j). To analyze *Shox2* and *Tbx4* expression in more detail, we performed in situ hybridization on adjacent limb sections from different developmental stages (Fig. 2B). The distinct proximal *Tbx4* expression domain of the E10.5 forelimb is consistent with that of *Sox9*, a marker for condensing mesenchyme, and overlaps with the broader *Shox2* expression domain (Fig. 2B a–c, arrowheads). From E11.5 onwards, the specific *Tbx4*-expressing region corresponds to a *Col2a1*-positive cartilaginous element of the dorsal forelimb (Fig. 2B d–i, arrowheads) and the expression patterns of *Shox2* and *Tbx4* are mutually exclusive. In the E10.5 and E11.5 hindlimb, *Shox2* and *Tbx4* expression broadly overlaps throughout the proximal limb mesenchyme (Fig. 2B a′–f′) and at E12.5 both are expressed in areas surrounding the proximal cartilaginous elements (Fig. 2B g′–i′, arrows).

To test whether *Tbx4* expression depends on Shox2 in the developing limbs, we carried out whole mount in situ hybridization (WISH) on WT and *Shox2*$^{-/-}$ embryos at 4 different developmental stages (Fig. 3A). These studies revealed that at E11.5, E12.5, and E13.5, *Tbx4* is upregulated in the specific dorsal *Tbx4*-expressing region of the mutant forelimb (Fig. 3A d, f, h). In all stages, hindlimb expression seems unaffected (data not shown). To quantify these findings, qRT-PCR was carried out using reverse transcribed RNA from separately dissected E10.5–E13.5 fore- and hindlimb tissue (Fig. 3B). As *Tbx4* is expressed specifically in the proximal region of the forelimb, only this part of the limb was dissected and used for the experiments. In accordance with the WISH results, no increase in *Tbx4* expression was detected at E10.5, but a significant increase in *Tbx4* expression in mutant forelimbs could be detected at E11.5, E12.5, and E13.5 (Fig. 3B b–d). Hindlimb expression was again largely unaffected at E10.5 to E12.5 and only slightly increased at E13.5 in *Shox2*$^{-/-}$ hindlimbs (Fig. 3B a–d). Thus, our analyses show that Shox2 has an inhibitory effect on *Tbx4* expression in the forelimbs during various developmental stages.

Tbx4 Regulates *Shox2* Expression in Developing Fore-and Hindlimbs

Considering that *Tbx4* is expressed earlier than *Shox2* in the limbs and that the regulation of *Tbx4* by Shox2 primarily affects the forelimb, we asked whether Tbx4 may also act as an upstream regulator of *Shox2*, which in turn signals back via a feedback mechanism. To investigate this possibility, we compared *Shox2* expression at E10.5 (when *Tbx4* expression starts in the forelimb) in WT and *Tbx4*$^{-/-}$ embryos. We can demonstrate that *Shox2* expression is reduced in both fore- and hindlimbs of *Tbx4*$^{-/-}$ embryos and that there is a stronger effect in the hindlimbs (Fig. 4A d, f). Quantification by qRT-PCR using separately dissected fore-and hindlimbs of E10.5 *Tbx4*-deficient mice revealed a significant reduction of *Shox2* expression in the fore- and hindlimb (Fig. 4B).

Tbx4 null mice initiate but do not continue hindlimb outgrowth and die at E10.5 due to chorioallantoic fusion defects (Naiche and Papaioannou, 2003). To address whether reduced *Shox2* expression may be caused by apoptosis, we carried out TUNEL analysis on WT and *Tbx4*$^{-/-}$ embryos at stage E10.5 and revealed that the apoptotic effect is minor (3.2% increase of apoptotic cells in the mutant forelimb and 9% in the mutant hindlimb; data not shown). In addition, siRNA-mediated knockdown experiments in primary embryonic fore-

and hindlimb cells isolated from WT embryos showed that *Shox2* is significantly down-regulated in fore- and hindlimb cells independent of apoptosis or aberrant limb formation (Fig. 4C). A nonspecific effect of the control siRNA on *Tbx4* or *Shox2* expression could be excluded (data not shown). Together, these data strongly support that Tbx4 acts as a transcriptional activator of *Shox2*.

Tbx4 Binds the *Shox2* Promoter

To investigate the transcriptional regulation of *Shox2* by Tbx4 on the promoter level, electrophoretic mobility shift assays (EMSA) were carried out. A ∼4 kb genomic upstream region of the murine *Shox2* transcriptional start site was examined for T-box binding sites by the MatInspector software tool (Genomatix Software GmbH) (Quandt et al., 1995; Cartharius et al., 2005). Specific Tbx4 binding sites are not known so far, but 3 binding sites for Brachyury, another T-box transcription factor, could be detected within a region of ∼3 kb. In addition, we identified 3 different sequences similar to the known TBX5-binding site (A/G)GGTGT(C/T/G)(A/G) (Ghosh et al., 2001) (Fig. 5A). As Tbx4 and Tbx5 are the most closely related of all known T-box proteins with an overall amino acid sequence homology of 52% and almost identical T-domains with 95% identity, we speculated that both proteins may share similar binding specificities, comparable to findings where Tbx4 was shown to be able to bind to the TBX5 binding site in the human *ANF* promoter (Arora et al., 2012). To determine if Tbx4 is able to interact directly with T-box binding sites in the murine *Shox2* promoter, EMSAs were performed using 6 different oligonucleotides containing the 3 Tbx5-like (T1–T3) and 3 Brachyury (B1–B3) binding sites (Fig. 5B). We show a specific binding of purified GST-tagged Tbx4 protein to the Tbx5-like oligo T3 but not to T1 or T2. There is also no binding to the Brachyury oligos B1–B3. To define the precise binding site, several nucleotides of the Tbx5 core binding sequence were mutated, which abolishes Tbx4 binding (Fig. 5B). In addition, competition assays show that excess of unlabelled Tbx5-like 3 (C-T3) decreases binding capability of GST-Tbx4 to labelled oligo Tbx5-like 3 (T3), whereas excess of mutated Tbx5-like 3 (C-T3 mut) has no effect (Fig. 5C).

Mutations in the *TBX4* and *TBX5* gene cause developmental syndromes associated with limb deformities in humans, known as small patella (*TBX4*) and Holt-Oram (*TBX5*) syndrome (Basson et al., 1997; Li et al., 1997; Bongers et al., 2004; McDermott et al., 2004). We investigated whether binding capacities of Tbx4 on the *Shox2* promoter also apply to the human system. In addition to 3 BRACHYURY binding sites (B1–B3), the human *SHOX2* promoter contains 3 sites matching known TBX5 binding elements (T1–T3, Fig. 6A). Human GST-tagged TBX4 protein interacts with all the 3 TBX5 binding sites (Fig. 6B) and binding is reduced upon addition of increasing amounts of unlabelled TBX5 binding site containing oligos (C-T1–3, Fig 6C). Consistent with the mouse data, there is no binding to the 3 BRACHYURY binding sites (Fig. 6B). Thus, TBX4/Tbx4 is able to bind the *SHOX2/Shox2* promoter in both human and mouse.

Discussion

To extend our knowledge of Shox2 functions during limb development, we searched for novel genes regulated by Shox2. We identified *Tbx4* as a particularly attractive candidate

that has essential functions in skeletal and muscular development of the hindlimbs, similar to *Shox2*. Making use of two different knockout mouse models, we validated a regulatory link of *Tbx4* and *Shox2* in developing limbs. Shox2 has a negative regulatory effect on *Tbx4* specifically in proximal forelimbs at developmental stages E11.5 to E13.5, but not in hindlimbs. This regulation can be matched to a distinct *Tbx4* expression domain within the cartilage of the dorsal forelimb where *Shox2* expression is normally excluded. Our data also revealed that Tbx4 activates *Shox2* in both fore- and hindlimbs, implicating Shox2 as a possible feedback modulator of *Tbx4* in the forelimb. The loss of the distinct proximal *Tbx4* expression in the forelimb results in a general downregulation of *Shox2* within the entire forelimb bud. To explain this observation, one could speculate that localized *Tbx4* expression in the WT forelimb induces upregulation of *Shox2* in nearby cells via a diffusible signaling molecule. In the absence of *Tbx4*, these cells fail to upregulate *Shox2* and stay in a more primitive state, which appears as a downregulation of *Shox2*. Considering equal expression of *Shox2* in fore- and hindlimbs, the observed forelimb restricted regulation of *Tbx4* by Shox2 was surprising. Interestingly, in a different study, *SHOX*, the highly related paralog of *SHOX2*, has been shown to completely rescue the *Shox2*$^{-/-}$ phenotype only in the forelimb, while the hindlimb defect persisted (Liu et al., 2011). A forelimb-specific corepressor of Shox2 acting in a temporal manner could explain this inhibitory effect on *Tbx4* expression from E11.5 onwards in the forelimb but not in the hindlimb. Together, these data strongly suggest that the genetic environment of limb-type-specific cofactors is important to mediate differential Shox2 effects in fore-and hindlimbs.

One interesting aspect is the biological significance of the *Shox2* regulatory effect on *Tbx4* in the defined proximal forelimb domain. Lineage tracing experiments revealed that *Tbx4*-expressing cells of this specific domain contribute mostly to the tendons around the elbow and to the periphery of the bone [Naiche et al., 2011). *Tbx4*-deficient mice had no apparent defects in gross forelimb morphology, yet the development of *Tbx4* mutant forelimb tendons was never examined in detail (Naiche and Papaioannou, 2007). The distinct expression of *Tbx4* in the forelimbs of mouse embryos was not found in Zebrafish pectoral fin buds or *Xenopus* forelimbs and only very low levels were seen during a single stage (stage 29) in the chicken wing (Gibson-Brown et al., 1998; Logan et al., 1998; Ruvinsky et al., 2000; Takabatake et al., 2000). These species-dependent expression differences could be the consequence of an enhancer element, which was shown previously to drive *Tbx4* forelimb expression in the mouse and is known to be poorly conserved in the other species (Menke et al., 2008). The regulation of *Tbx4* by Shox2 may therefore contribute to the development of distinct tendons and bone elements particularly in the developing mammalian forelimb.

We have provided evidence that Tbx4 regulates *Shox2*. *Tbx4* is already strongly expressed in the lateral plate mesoderm at E9.5 prior to hindlimb bud outgrowth, when *Shox2* expression begins. We show that Tbx4 is an activator of *Shox2* in both limb types, which is in contrast to the forelimb-specific inhibition of *Tbx4* by Shox2. In addition to its early function in limb outgrowth, Tbx4 is also crucial for the development of hindlimb skeletal elements as well as muscle and tendons during a second later phase of limb formation (Naiche and Papaioannou, 2003, 2007; Hasson et al., 2010). The deletion of *Tbx4* in mouse shortly after hindlimb initiation leads to abnormal pelvises and severely hypoplastic femurs. This phenotype

resembles the drastically shortened humerus and femur as well as the mildly abnormal pelvic girdle caused by *Shox2* deficiency (Cobb et al., 2006; Yu et al., 2007) (Fig. 1). In addition to the skeletal malformations, the conditional loss of *Tbx4* results in disturbed limb muscle patterning, size, and orientation (Hasson et al., 2010). Interestingly, altered muscle patterning with reorientated and abnormal muscle bundles was also reported in *Shox2*-deficient mice (Vickerman et al., 2011), suggesting that *Tbx4* and Shox2 share critical functions during limb development. Compared to the *Tbx4* mutant phenotype, however, in the *Shox2* mutant fewer muscles are affected and defects are restricted to the proximal part of the limbs. Thus, the loss of either gene, *Tbx4* or *Shox2*, leads to a phenotype in skeletal and muscular elements.

The gene pair *Tbx4* and *Tbx5* originated from a common ancestral gene by tandem duplication and both genes have almost identical T-box domains (Agulnik et al., 1996). Overlapping binding and regulative properties are therefore conceivable. We have shown that Tbx4 is able to bind to a sequence motif very similar to known Tbx5 binding motifs within the murine *Shox2* promoter. A specific interaction of TBX4 with three TBX5 binding sites in the human promoter region has also been demonstrated, suggesting that the regulation of *SHOX2* by TBX4 also plays a role in human limb development and limb-associated diseases. Tbx4 is capable of compensating for a loss of Tbx5 function in the forelimbs (Minguillon et al., 2005) and both proteins transactivate the same reporter containing T-box binding elements via a shared activator domain (Ouimette et al., 2010). Considering this and the fact that Tbx5 acts as an upstream regulator of *Shox2* during heart development (Puskaric et al., 2010), one can hypothesize that Tbx5 is the Tbx4 corresponding regulator of *Shox2* in the forelimb controlling muscle and skeleton development. Simultaneously, Tbx4 activates *Shox2*, probably in a feedback loop, contributing to forelimb tendon and bone formation.

During limb development, only a small number of genes are differentially expressed in either fore- or hindlimbs including specific members of the T-box family (Gibson-Brown et al., 1996). The vast majority of genes playing a role in limb formation including *Shox2* are equally expressed in both limb structures (Blaschke et al., 1998; Semina et al., 1998; Zeller et al., 2009). Our study demonstrates that genes expressed at similar abundance in both limb types (e.g. *Shox2*) can be activated by genes distinctly expressed in fore- and hindlimbs (e.g. *Tbx4*). In turn, a gene expressed in both fore- and hindlimb can have a regulatory effect on a target gene specifically expressed in only one limb type.

Experimental Procedures

Mice and Tissue Collection

Mice used were *Shox2*$^{-/-}$ (Blaschke et al., 2007) and *Tbx4*$^{-/-}$ (Naiche and Papaioannou, 2003). For maximum litter size, we crossed the *Shox2*$^{-/-}$ mice into the CD-1 outbred strain. Breeding and genotyping was performed as previously described (Naiche and Papaioannou, 2003; Blaschke et al., 2007) and detection of the mating plug was considered 0.5 days post conception (E0.5). For E12.5 microarray analysis, isolated fore- and hindlimbs were combined; for E11.5 microarray analysis and quantitative RT-PCR (qRT-PCR), they were analyzed separately. Limb buds from littermates of the same genotype were pooled and total

RNA was purified using TRIzol® (Invitrogen, Carlsbad, CA) extraction. For in situ hybridization, isolated embryos or limbs were fixed in 4% paraformaldehyde at 4° C overnight, dehydrated in methanol and stored at −20° C (whole mount in situ hybridization), or incubated in 30% sucrose at 4° C overnight and embedded in tissue freezing medium (Jung) (section in situ hybridization).

Histological Stainings

Alcian Blue/Alizarin Red stainings of E16.5 skeletal preparations were performed according to standard protocols (Nagy et al., 2003). An Alcian Blue solution containing 150 mg Alcian Blue 8 GX (Sigma, St. Louis, MO)/l in 95% Ethanol, 20% acetic acid, and an Alizarin Red solution containing 50 mg Alizarin Red (Sigma)/l and 10 g KOH/l was used.

Microarray Hybridization and Analysis

Gene expression profiling was carried out using oligonucleotide arrays of the MoGene 2.0 ST (E11.5)- and Mouse Genome 430 2.0 (E12.5)-type from Affymetrix (Santa Clara, CA) according to the manufacturer's protocol. For E11.5, forelimb RNA from 3–4 embryos of 2 different litters was used for hybridization to 2 arrays per genotype (WT and *Shox2*$^{-/-}$). For E12.5, combined fore- and hindlimb RNA from 3–4 embryos of 2 different litters was pooled and used for hybridization to 1 array per genotype. RNA quality was confirmed by the Agilent 2100 Bioanalyzer (Agilent Technologies, Santa Clara, CA) and 200 ng was used to generate biotinylated ssDNA followed by hybridization to arrays. Statistical comparisons of WT and *Shox2*$^{-/-}$ chip data were performed using the software package JMP Genomics, version 4.0 from SAS (SAS Institute, Cary, NC). Values of perfect-matches were log transformed, quantile normalised, and fitted with log-linear mixed models, with probe ID and genotype considered to be constant. A custom CDF version 11 (E12.5) and version 17 [E11.5) with UniGene-based gene definitions was used to annotate the arrays. The microarray data were deposited in the NCBI GEO database with accession number GSE51523 (for E11.5 arrays) and GSE41945 (for E12.5 arrays).

DNA Constructs

To generate RNA antisense probes for in situ hybridization, 607 bp (*Tbx4*, accession number NM_011536.2), 654 bp (*Col2a1*, accession number NM_031163.3), and 637 bp (*Sox9*, accession number NM_011448.4) of the mRNA sequence were amplified by PCR using the primers Tbx4 ISH for2/rev2, Col2a1 ISH for/rev, Sox9 ISH for/rev (Table 1) and mouse E12.5 hindlimb cDNA. The PCR products were then subcloned into the pSTBlue1 vector (Novagen, Madison, WI). The plasmid pCR-S-Og12 for generation of the *Shox2* mRNA antisense probe was described previously (Blaschke et al., 1998). GST-*Tbx4*/GST-*TBX4* expression vectors for EMSA were generated by amplifying the mouse/human *Tbx4/TBX4* coding sequence (accession number NM_018488.2/NM_011536.2) using cDNA from E12.5 primary mouse hindlimb cells and normal human dermal fibroblasts (NHDF), respectively. Subsequently, *Tbx4/TBX4* was subcloned via *BamHI/HindIII* (mouse) and *HindIII/XhoI* (human) into pET-41a(+) vector (Novagen). All primer sequences used for cloning are listed in Table 1.

In Situ Hybridization

Riboprobe generation and whole mount in situ hybridization on mouse embryos were performed as reported (Harland, 1991). Digoxigenin-labeled antisense (as) and sense (s) RNA was synthesized from the plasmids pCR-S-*Og12* (*Shox2*, linearized by *SacI*(as)/*XhoI* (s) and transcribed using T7 (as)/T3 (s) polymerase), pSTBlue1-*Tbx4* (linearized by *MluI* (as)/*HindIII* (s) and transcribed using SP6 (as)/T7 (s) polymerase), pSTBlue1-*Col2a1* (linearized by *KpnI* (as)/*HindIII* (s) and transcribed using SP6 (as)/T7 (s) polymerase) and pSTBlue1-*Sox9* (linearized by *HindIII* (as)/*KpnI* (s) and transcribed using T7 (as)/SP6 (s) polymerase). Section in situ hybridization on adjacent 12 μm cryosections was performed as described previously (Decker et al., 2011).

cDNA Synthesis and Quantitative RT-PCR

1 μg of total RNA was transcribed into cDNA by SuperScript™ First-Strand Synthesis System for RT-PCR (Invitrogen). qRT-PCR was performed using the Applied Biosystems 7500 Real-Time PCR System and SYBR Green ROX dye (Thermo Scientific, Waltham, MA). Each of the samples was analyzed in duplicate and relative mRNA levels were assessed according to the delta-delta C_t method (Pfaffl, 2001) by normalization to succinate dehydrogenase complex subunit A (*Sdha*) and hypoxanthine phosphoribosyltransferase 1 (*Hprt1*). All qRT-PCR primer sequences are listed in Table 1.

Apoptosis Detection

Apoptotic cells in the limb region of E10.5 WT and $Tbx4^{-/-}$ embryos were visualized by TUNEL staining using an in situ cell death detection kit (TMR red, Roche, Indianapolis, IN) according to the manufacturer's instructions. TUNEL staining was performed on transverse 10 μm cryosections of E10.5 embryos and sections were counterstained using Hoechst (Invitrogen); 3–8 different fore- and hindlimb sections per embryo from in total 4 embryos per genotype (WT and $Tbx4^{-/-}$, n=4) were used. Apoptotic cells and Hoechst-stained cells were counted using the analyze particles tool from ImageJ and the number of apoptotic cells was normalized to the whole cell number.

Limb Cell Culture and Transfection

Limb buds (fore- and hindlimbs separately) were dissected at E12.5, dissociated mechanically (using forceps) and subsequently enzymatically (using 0.5% Trypsin-EDTA from Gibco, Gaithersburg, MD), and plated on cell culture dishes coated with 0.1% gelatine in PBS. Cells were cultured in DMEM (Dulbecco's modified Eagle's medium; Gibco) containing 10% FBS (fetal bovine serum gold; PAA), 1% penicillin/streptomycin (Gibco), 1% L-glutamine (Gibco), and 1% NEAA (non-essential amino acids; Gibco) at 37°C, 5% CO_2 and 95% humidity. For knockdown experiments, cells were seeded in 6-well plates and transfected with 40 pmol/well of *Tbx4* silencer select siRNA (Invitrogen) #1 (ID S18204), siRNA #2 (ID 74781), or control siRNA by using RNAiMax (Invitrogen). Cells were harvested 24 hr after transfection for qRT-PCR.

Electrophoretic Mobility Shift Assay (EMSA)

To identify T-box binding sites within the *Shox2/SHOX2* promotor, a ∼4 kb genomic upstream region of the transcriptional start site was examined using the MatInspector software tool (Genomatix Software GmbH) (Quandt et al., 1995; Cartharius et al., 2005). The murine *Shox2* promoter region contained 3 Brachyury binding sites with the core sequence T(G/C)ACACCT/AGGTGTGAAATT (Kispert and Hermann, 1993; Ghosh et al., 2001) (Brachyury 1 [−4,856 bp/−4,841 bp], Brachyury 2 [−3,158 bp/−3,143 bp], Brachyury 3 [−2,089 bp/−2,074 bp]) and additionally we identified 3 different sequences similar to known Tbx5 binding sites with the core sequence (A/G)GGTGT(C/T/G)(A/G) (Ghosh et al., 2001) (Tbx5-like 1 [−3,623 bp/−3,616 bp], Tbx5-like 2 [−2,707 bp/−2,700 bp] and Tbx5-like 3 [−2,341 bp/−2,348 bp]). The human *SHOX2* promoter region contained 3 BRACHYURY (BRACHYURY 1 [−2,598 bp/−2,583 bp], BRACHYURY 2 [−2,227 bp/−2,211 bp], BRACHYURY 3 [−1,745 bp, −1,730 bp]) and 3 TBX5 (TBX5 1 [−4,054 bp/−4,049 bp], TBX5 2 [−3,690bp/−3,685 bp] and TBX5 3 [−2,482 bp/−2,477 bp]) binding sites.

EMSA was performed as reported previously (Schneider et al. 2005). For the binding reaction, ^{32}P-labelled, 60-bp double stranded mouse *Shox2* oligonucleotides (Oligo T1 [−3,647 bp/−3,576 bp]; Oligo T2 [−2,730 bp/−2,671 bp]; T3 [−2,376 bp/−2,317 bp]; B1 [−4,879 bp/−4,820 bp]; B2 [−3,180 bp/−3,121 bp; B3 [−2,111 bp/2,052 bp]; Table 1) and human *SHOX2* oligonucleotides (Oligo T1 [−4,084 bp/−4,023 bp]; Oligo T2 [−3,719 bp/−3,658 bp]; Oligo T3 [−2,511 bp/−2,450 bp]; Oligo B1 [−2,620 bp/−2,560 bp]; Oligo B2 [−2,249 bp/−2,188 bp]; Oligo B3 [−2,511 bp/−2,450 bp]; Table 1), were used together with purified, bacterially expressed recombinant GST-Tbx4/GST-TBX4 protein.

Statistical Analysis

Results of qRT-PCR are presented as mean ± SEM from at least 3 independent experiments. Experimental group comparisons were performed using the Student's *t*-test and differences were considered significant if $P < 0.05$.

Supplementary Material

Refer to Web version on PubMed Central for supplementary material.

Acknowledgments

We thank Maria Muciek and Carsten Sticht for help with the microarray analysis and Roland Knopf for animal care.

Grant sponsor: Deutsche Forschungsgemeinschaft; Grant number: RA 380/12-1.

References

Agarwal P, Wylie JN, Galceran J, Arkhitko O, Li C, Deng C, Grosschedl R, Bruneau BG. Tbx5 is essential for forelimb bud initiation following patterning of the limb field in the mouse embryo. Development. 2003; 130:623–633. [PubMed: 12490567]

Agulnik SI, Garvey N, Hancock S, Ruvinsky I, Chapman DL, Agulnik I, Bollag R, Papaioannou V, Silver LM. Evolution of mouse T-box genes by tandem duplication and cluster dispersion. Genetics. 1996; 144:249–254. [PubMed: 8878690]

Arora R, Del Alcazar CM, Morrisey EE, Naiche LA, Papaioannou VE. Candidate gene approach identifies multiple genes and signaling pathways downstream of tbx4 in the developing allantois. PLoS One. 2012; 7:e43581. [PubMed: 22952711]

Basson CT, Bachinsky DR, Lin RC, Levi T, Elkins JA, Soults J, Grayzel D, Kroumpouzou E, Traill TA, Leblanc-Straceski J, Renault B, Kucherlapati R, Seidman JG, Seidman CE. Mutations in human TBX5 [corrected] cause limb and cardiac malformation in Holt-Oram syndrome. Nat Genet. 1997; 15:30–35. [PubMed: 8988165]

Belin V, Cusin V, Viot G, Girlich D, Toutain A, Moncla A, Vekemans M, Le Merrer M, Munnich A, Cormier-Daire V. SHOX mutations in dyschondrosteosis (Leri-Weill syndrome). Nat Genet. 1998; 19:67–69. [PubMed: 9590292]

Benito-Sanz S, Thomas NS, Huber C, Gorbenko del Blanco D, Aza-Carmona M, Crolla JA, Maloney V, Rappold G, Argente J, Campos-Barros A, Cormier-Daire V, Heath KE. A novel class of Pseudoautosomal region 1 deletions downstream of SHOX is associated with Leri-Weill dyschondrosteosis. Am J Hum Genet. 2005; 77:533–544. [PubMed: 16175500]

Blaschke RJ, Monaghan AP, Schiller S, Schechinger B, Rao E, Padilla-Nash H, Ried T, Rappold GA. SHOT, a SHOX-related homeobox gene, is implicated in craniofacial, brain, heart, and limb development. Proc Natl Acad Sci USA. 1998; 95:2406–2411. [PubMed: 9482898]

Blaschke RJ, Hahurij ND, Kuijper S, Just S, Wisse LJ, Deissler K, Maxelon T, Anastassiadis K, Spitzer J, Hardt SE, Scholer H, Feitsma H, Rottbauer W, Blum M, Meijlink F, Rappold G, Gittenberger-de Groot AC. Targeted mutation reveals essential functions of the homeodomain transcription factor Shox2 in sinoatrial and pacemaking development. Circulation. 2007; 115:1830–1838. [PubMed: 17372176]

Bongers EM, Duijf PH, van Beersum SE, Schoots J, Van Kampen A, Burckhardt A, Hamel BC, Losan F, Hoefsloot LH, Yntema HG, Knoers NV, van Bokhoven H. Mutations in the human TBX4 gene cause small patella syndrome. Am J Hum Genet. 2004; 74:1239–1248. [PubMed: 15106123]

Boulet AM, Capecchi MR. Multiple roles of Hoxa11 and Hoxd11 in the formation of the mammalian forelimb zeugopod. Development. 2004; 131:299–309. [PubMed: 14668414]

Cartharius K, Freeh K, Grote K, Klocke B, Haltmeier M, Klingenhoff A, Frisch M, Bayerlein M, Werner T. Matlnspector and beyond: promoter analysis based on transcription factor binding sites. Bioinformatics. 2005; 21:2933–2942. [PubMed: 15860560]

Chapman DL, Garvey N, Hancock S, Alexiou M, Agulnik SI, Gibson-Brown JJ, Cebra-Thomas J, Bollag RJ, Silver LM, Papaioannou VE. Expression of the T-box family genes, Tbx1-Tbx5, during early mouse development. Dev Dyn. 1996; 206:379–390. [PubMed: 8853987]

Chen J, Wildhardt G, Zhong Z, Roth R, Weiss B, Steinberger D, Decker J, Blum WF, Rappold G. Enhancer deletions of the SHOX gene as a frequent cause of short stature: the essential role of a 250 kb downstream regulatory domain. J Med Genet. 2009; 46:834–839. [PubMed: 19578035]

Cobb J, Dierich A, Huss-Garcia Y, Duboule D. A mouse model for human short-stature syndromes identifies Shox2 as an upstream regulator of Runx2 during long-bone development. Proc Natl Acad Sci USA. 2006; 103:4511–4515. [PubMed: 16537395]

Davis AP, Witte DP, Hsieh-Li HM, Potter SS, Capecchi MR. Absence of radius and ulna in mice lacking hoxa-11 and hoxd-11. Nature. 1995; 375:791–795. [PubMed: 7596412]

Decker E, Durand C, Bender S, Rodelsperger C, Glaser A, Hecht J, Schneider KU, Rappold G. FGFR3 is a target of the homeobox transcription factor SHOX in limb development. Hum Mol Genet. 2011; 20:1524–1535. [PubMed: 21273290]

Duboc V, Logan MP. Regulation of limb bud initiation and limb-type morphology. Dev Dyn. 2011; 240:1017–1027. [PubMed: 21360788]

Ghosh TK, Packham EA, Bonser AJ, Robinson TE, Cross SJ, Brook JD. Characterization of the TBX5 binding site and analysis of mutations that cause Holt-Oram syndrome. Hum Mol Genet. 2001; 10:1983–1994. [PubMed: 11555635]

Gibson-Brown JJ, Agulnik SI, Chapman DL, Alexiou M, Garvey N, Silver LM, Papaioannou VE. Evidence of a role for T-box genes in the evolution of limb morphogenesis and the specification of forelimb/hindlimb identity. Mech Dev. 1996; 56:93–101. [PubMed: 8798150]

Gibson-Brown JJ, Agulnik SI, Silver LM, Niswander L, Papaioannou VE. Involvement of T-box genes Tbx2-Tbx5 in vertebrate limb specification and development. Development. 1998; 125:2499–2509. [PubMed: 9609833]

Gross S, Krause Y, Wuelling M, Vortkamp A. Hoxa11 and hoxd11 regulate chondrocyte differentiation upstream of runx2 and shox2 in mice. PLoS One. 2012; 7:e43553. [PubMed: 22916278]

Harland RM. In situ hybridization: an improved whole-mount method for Xenopus embryos. Methods Cell Biol. 1991; 36:685–695. [PubMed: 1811161]

Hasson P, DeLaurier A, Bennett M, Grigorieva E, Naiche LA, Papaioannou VE, Mohun TJ, Logan MP. Tbx4 and tbx5 acting in connective tissue are required for limb muscle and tendon patterning. Dev Cell. 2010; 18:148–156. [PubMed: 20152185]

Kispert A, Hermann BG. The Brachyury gene encodes a novel DNA binding protein. EMBO J. 1993; 12:4898–4899. [PubMed: 8223498]

Kronenberg HM. Developmental regulation of the growth plate. Nature. 2003; 423:332–336. [PubMed: 12748651]

Li QY, Newbury-Ecob RA, Terrett JA, Wilson Dl, Curtis AR, Yi CH, Gebuhr T, Bullen PJ, Robson SC, Strachan T, Bonnet D, Lyonnet S, Young ID, Raeburn JA, Buckler AJ, Law DJ, Brook JD. Holt-Oram syndrome is caused by mutations in TBX5, a member of the Brachyury (T) gene family. Nat Genet. 1997; 15:21–29. [PubMed: 8988164]

Liu H, Chen CH, Espinoza-Lewis RA, Jiao Z, Sheu I, Hu X, Lin M, Zhang Y, Chen Y. Functional redundancy between human SHOX and mouse Shox2 genes in the regulation of sinoatrial node formation and pacemaking function. J Biol Chem. 2011; 286:17029–17038. [PubMed: 21454626]

Logan M, Simon HG, Tabin C. Differential regulation of T-box and homeobox transcription factors suggests roles in controlling chick limb-type identity. Development. 1998; 125:2825–2835. [PubMed: 9655805]

Mariani FV, Martin GR. Deciphering skeletal patterning: clues from the limb. Nature. 2003; 423:319–325. [PubMed: 12748649]

McDermott, DA.; Fong, JC.; Basson, CT. Holt-Oram Syndrome. Seattle: Gene Reviews; 2004.

Menke DB, Guenther C, Kingsley DM. Dual hindlimb control elements in the Tbx4 gene and region-specific control of bone size in vertebrate limbs. Development. 2008; 135:2543–2553. [PubMed: 18579682]

Minguillon C, Del Buono J, Logan MP. Tbx5 and Tbx4 are not sufficient to determine limb-specific morphologies but have common roles in initiating limb outgrowth. Dev Cell. 2005; 8:75–84. [PubMed: 15621531]

Nagy, A.; Gertsenstein, M.; Vintersten, K.; Behringer, R. Manipulating the mouse embryo. Cold Spring Harbor, NY: Cold Spring Habor Laboratory Press; 2003.

Naiche LA, Papaioannou VE. Loss of Tbx4 blocks hindlimb development and affects vascularization and fusion of the allan-tois. Development. 2003; 130:2681–2693. [PubMed: 12736212]

Naiche LA, Papaioannou VE. Tbx4 is not required for hindlimb identity or post-bud hindlimb outgrowth. Development. 2007; 134:93–103. [PubMed: 17164415]

Naiche LA, Arora R, Kania A, Lewandoski M, Papaioannou VE. Identity and fate of Tbx4-expressing cells reveal developmental cell fate decisions in the allantois, limb, and external genitalia. Dev Dyn. 2011; 240:2290–2300. [PubMed: 21932311]

Ng JK, Kawakami Y, Buscher D, Raya A, Itoh T, Koth CM, Rodriguez Esteban C, Rodriguez-Leon J, Garrity DM, Fishman MC, Izpisua Belmonte JC. The limb identity gene Tbx5 promotes limb initiation by interacting with Wnt2b and Fgf10. Development. 2002; 129:5161–5170. [PubMed: 12399308]

Ouimette JF, John ML, L'Honore A, Gifuni A, Drouin J. Divergent transcriptional activities determine limb identity. Nat Commun. 2010; 1:35. [PubMed: 20975709]

Pearse RV 2nd, Scherz PJ, Campbell JK, Tabin CJ. A cellular lineage analysis of the chick limb bud. Dev Biol. 2007; 310:388–400. [PubMed: 17888899]

Pfaffl MW. A new mathematical model for relative quantification in real-time RT-PCR. Nucleic Acids Res. 2001; 29:e45. [PubMed: 11328886]

Puskaric S, Schmitteckert S, Mori AD, Glaser A, Schneider KU, Bruneau BG, Blaschke RJ, Steinbeisser H, Rappold G. Shox2 mediates Tbx5 activity by regulating Bmp4 in the pacemaker region of the developing heart. Hum Mol Genet. 2010; 19:4625–4633. [PubMed: 20858598]

Quandt K, Frech K, Karas H, Wingender E, Werner T. MatInd and MatInspector: new fast and versatile tools for detection of consensus matches in nucleotide sequence data. Nucleic Acids Res. 1995; 23:4878–4884. [PubMed: 8532532]

Rallis C, Bruneau BG, Del Buono J, Seidman CE, Seidman JG, Nissim S, Tabin CJ, Logan MP. Tbx5 is required for fore-limb bud formation and continued outgrowth. Development. 2003; 130:2741–2751. [PubMed: 12736217]

Rosilio M, Huber-Lequesne C, Sapin H, Carel JC, Blum WF, Cormier-Daire V. Genotypes and phenotypes of children with SHOX deficiency in France. J Clin Endocrinol Metab. 2012; 97:E1257–E1265. [PubMed: 22518848]

Ruvinsky I, Oates AC, Silver LM, Ho RK. The evolution of paired appendages in vertebrates: T-box genes in the zebrafish. Dev Genes Evol. 2000; 210:82–91. [PubMed: 10664151]

Schiller S, Spranger S, Schechinger B, Fukami M, Merker S, Drop SL, Troger J, Knoblauch H, Kunze J, Seidel J, Rappold GA. Phenotypic variation and genetic heterogeneity in Leri-Weill syndrome. Eur J Hum Genet. 2000; 8:54–62. [PubMed: 10713888]

Schneider KU, Marchini A, Sabherwal N, Roth R, Niesler B, Marttila T, Blaschke RJ, Lawson M, Dumic M, Rappold G. Alteration of DNA binding, dimerization, and nuclear translocation of SHOX homeodomain mutations identified in idiopathic short stature and Leri-Weill dyschondrosteosis. Hum Mutat. 2005; 26:44–52. [PubMed: 15931687]

Semina EV, Reiter RS, Murray JC. A new human homeobox gene OGI2X is a member of the most conserved homeobox gene family and is expressed during heart development in mouse. Hum Mol Genet. 1998; 7:415–422. [PubMed: 9466998]

Shears DJ, Vassal HJ, Goodman FR, Palmer RW, Reardon W, Superti-Furga A, Scambler PJ, Winter RM. Mutation and deletion of the pseudoautosomal gene SHOX cause Leri-Weill dyschondrosteosis. Nat Genet. 1998; 19:70–73. [PubMed: 9590293]

Takabatake Y, Takabatake T, Takeshima K. Conserved and divergent expression of T-box genes Tbx2-Tbx5 in Xenopus. Mech Dev. 2000; 91:433–437. [PubMed: 10704879]

Vickerman L, Neufeld S, Cobb J. Shox2 function couples neural, muscular and skeletal development in the proximal fore-limb. Dev Biol. 2011; 350:323–336. [PubMed: 21156168]

Wellik DM, Capecchi MR. Hox10 and Hox11 genes are required to globally pattern the mammalian skeleton. Science. 2003; 301:363–367. [PubMed: 12869760]

Yu L, Liu H, Yan M, Yang J, Long F, Muneoka K, Chen Y. Shox2 is required for chondrocyte proliferation and maturation in proximal limb skeleton. Dev Biol. 2007; 306:549–559. [PubMed: 17481601]

Zeller R, Lopez-Rios J, Zuniga A. Vertebrate limb bud development: moving towards integrative analysis of organogenesis. Nat Rev Genet. 2009; 10:845–858. [PubMed: 19920852]

Zinn AR, Wei F, Zhang L, Elder FF, Scott CI Jr, Marttila P, Ross JL. Complete SHOX deficiency causes Langer mesomelic dysplasia. Am J Med Genet. 2002; 110:158–163. [PubMed: 12116254]

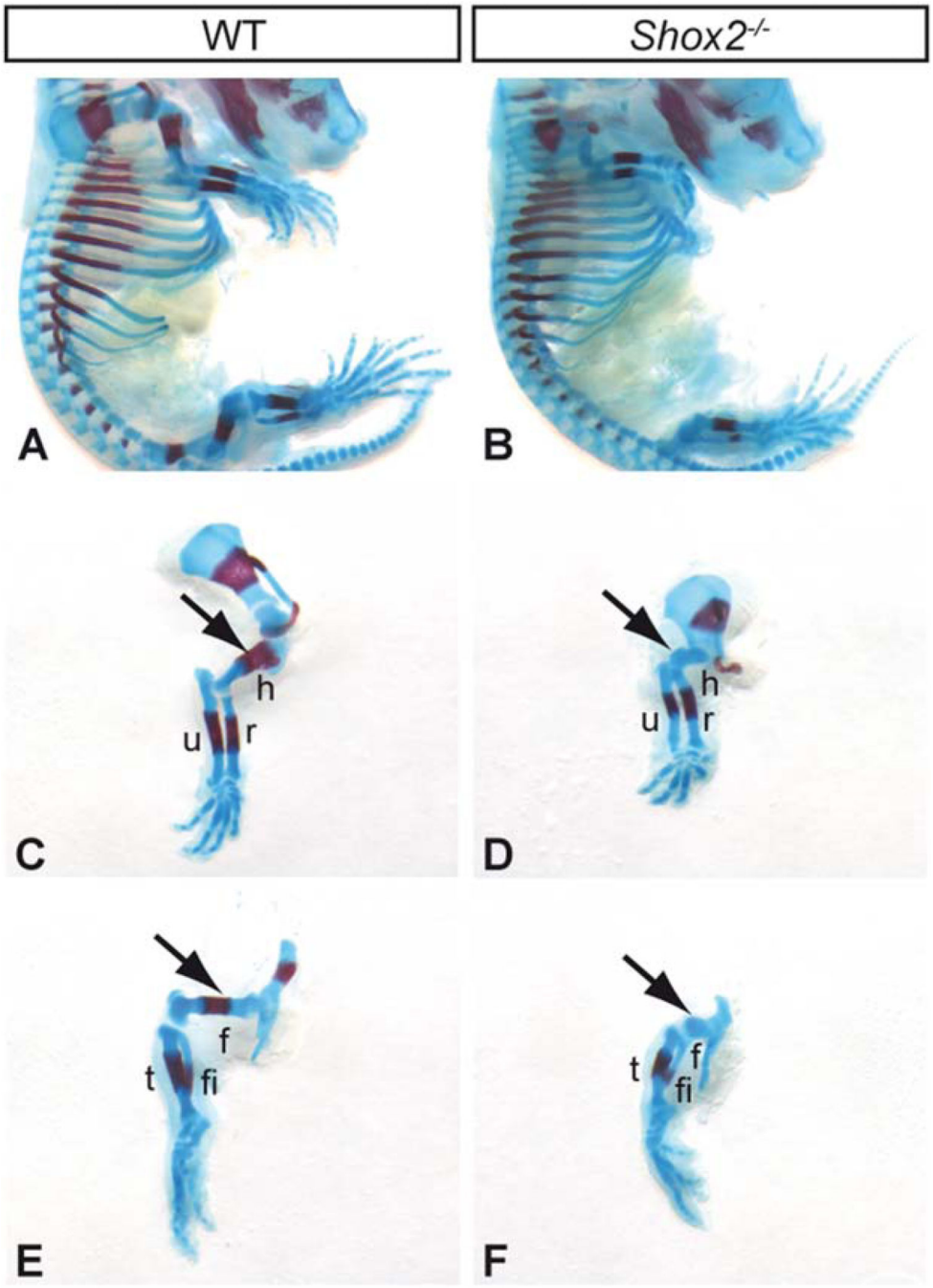

Fig. 1.

Shox2 deficiency results in shortened limbs. Alizarin red (bone, red) - Alcian blue (cartilage, blue) staining on E16.5 WT (**A**) and *Shox2* mutant (**B**) embryos revealed a severe shortening of *Shox2* mutant fore-(**D**) and hindlimbs (**F**) compared to the wildtype (**C, E**). The proximal skeletal elements humerus and femur are particularly affected and show no ossification (arrows). The more distal parts of the *Shox2*$^{-/-}$ limbs (radius, ulna, tibia, and fibula) are only slightly shortened compared to the wildtype. h, humerus; r, radius; f, femur; fi, fibula; t, tibia; u, ulna.

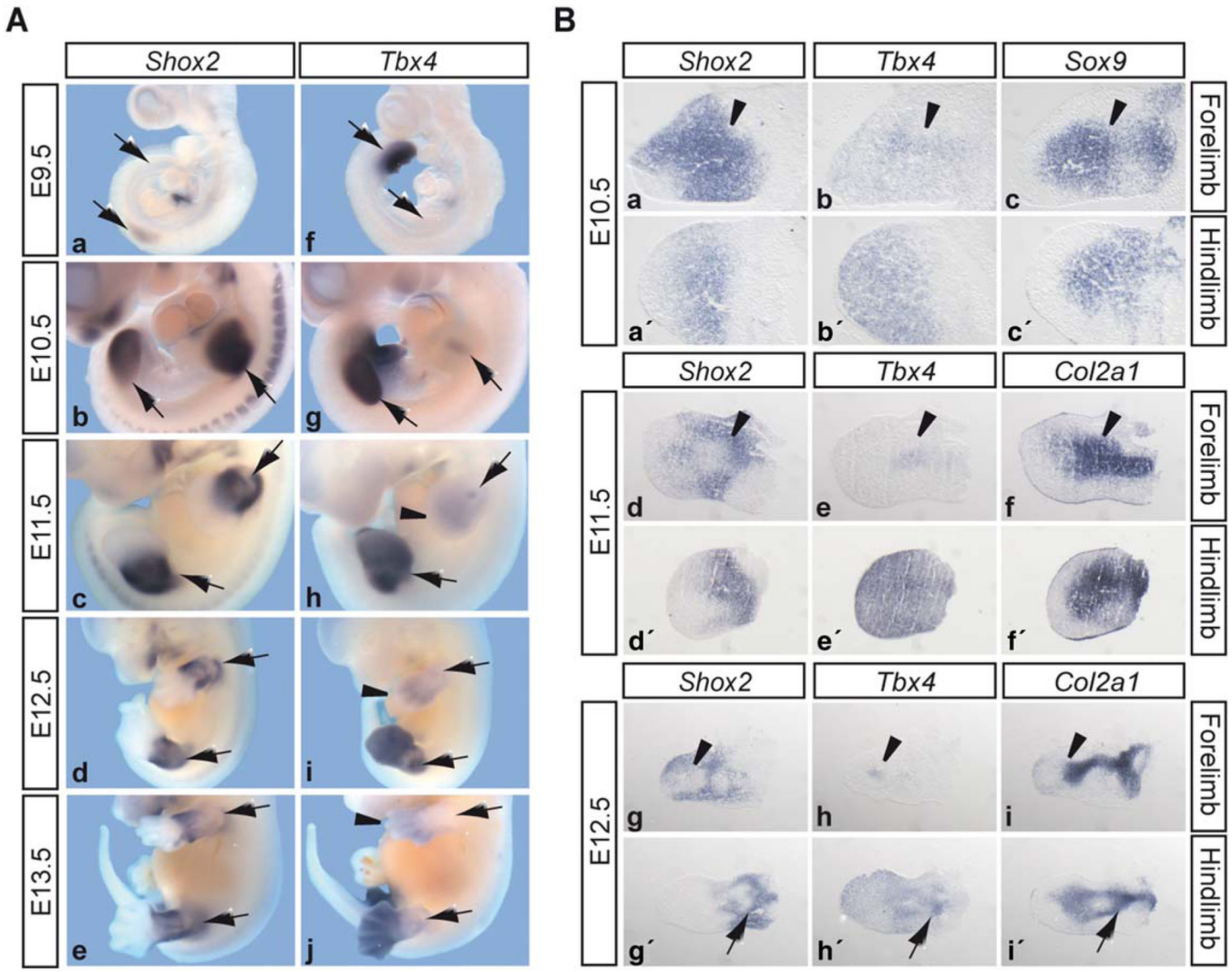

Fig. 2.

Shox2 and *Tbx4* expression during murine limb development. **A:** Whole mount in situ hybridization on mouse embryos of different developmental stages (limbs or limb developing regions are indicated by arrows). *Shox2* expression starts at E9.5 in the forelimb buds (a), is expressed throughout fore- and hindlimb buds at E10.5 (**b**), and from E11.5–E13.5 restricted to the proximal part of the limbs (**c–e**). *Tbx4* hindlimb expression starts at E9.5 in the lateral plate mesoderm (**f**), continues throughout E10.5–E12.5 (**g–i**), and restricts distally at E13.5 (**j**). In the forelimbs, distinct *Tbx4* staining is visible at E10.5-E12.5 (**g–i**). In addition, a diffuse *Tbx4* expression can be seen at E11.5 (h, arrowhead), which again restricts distally from E12.5 onward (i, j, arrowheads). B: In situ hybridization on 12 μm adjacent limb sections of different developmental stages. Dorsal sections of the forelimb (**a–i**) and medial sections of the hindlimbs (**a′-i′**) are presented. The *Tbx4* expression domain of the forelimb and the corresponding *Shox2* expression are indicated at E10.5 (a, b), E11.5 (d, e), and E12.5 (g, h) by arrowheads. *Sox9* and *Col2a1* were used as markers for condensing mesenchyme, and cartilaginous skeletal elements, respectively. Hindlimb expression of

Shox2 (g′) and *Tbx4* (h′) surrounding the cartilaginous elements at E12.5 are indicated by arrows.

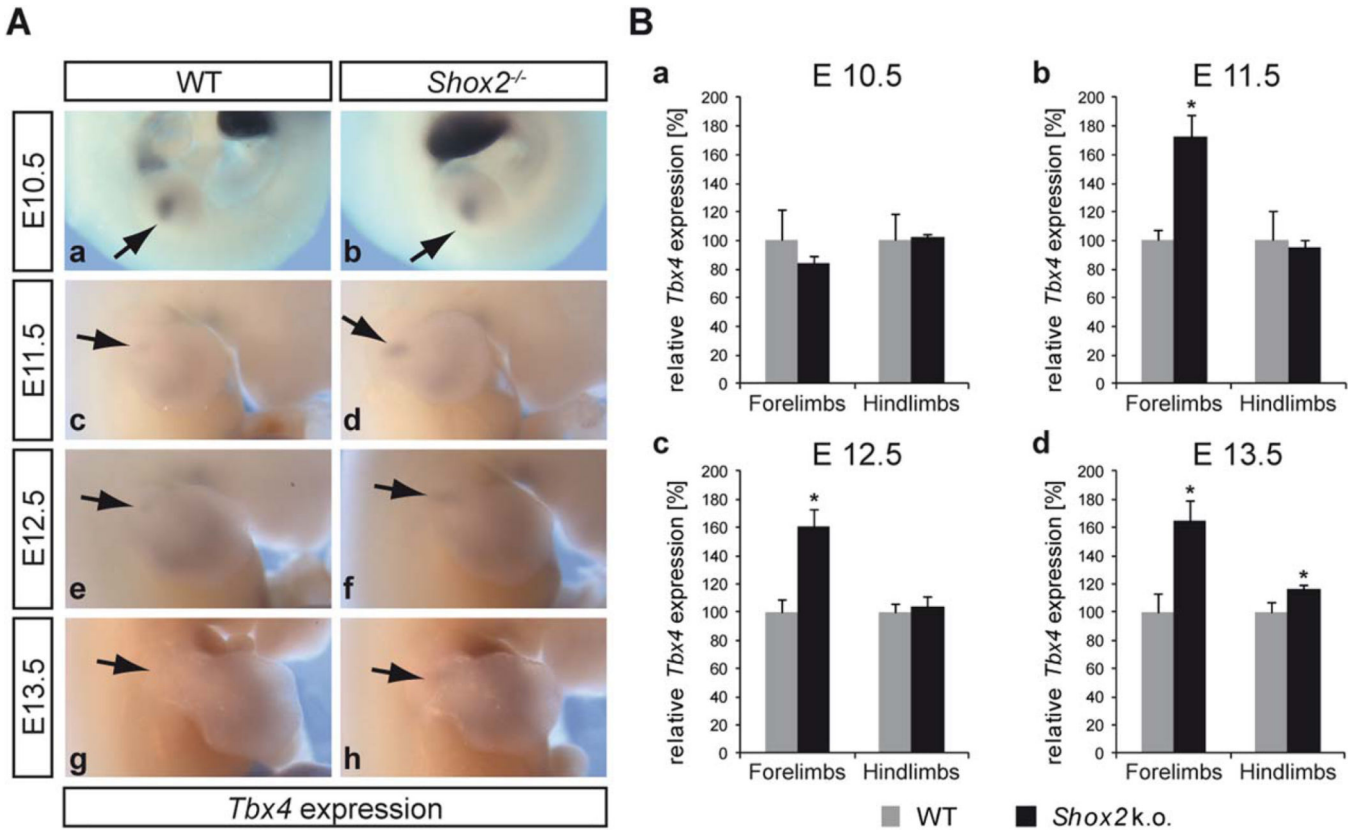

Fig. 3.

Tbx4 is upregulated in *Shox2*$^{-/-}$ forelimbs. **A:** Whole mount in situ hybridisation on WT and *Shox2*$^{-/-}$ embryos using a *Tbx4* RNA probe shows no altered expression of *Tbx4* in E10.5 *Shox2*$^{-/-}$ forelimbs (**b**), but an upregulation of *Tbx4* in E11.5 (**d**), E12.5 (**f**), and E13.5 (h) forelimbs compared to the WT (**a, c, e, g**), indicated by arrows; n = 3 independent stainings for every stage, each performed with 2–3 littermates per genotype. B: Quantification by qRT-PCR using WT and *Shox2*$^{-/-}$ limb tissue. *Shox2* deficiency results in a significant increase of *Tbx4* mRNA (~60– 70%) in E11.5 (b), E12.5 (c), and E13.5 (d) forelimbs. Hindlimb expression is largely unaffected at E10.5 to E12.5 (**a**–**c**) and only slightly elevated at E13.5 **(d)**. Significance is indicated by asterisks: *$P \leq 0.05$; n = 3 independent experiments for every stage, each performed with 2–7 littermates per genotype; grey bars indicate relative *Tbx4* mRNA levels in WT, black bars relative *Tbx4* mRNA levels in *Shox2*$^{-/-}$.

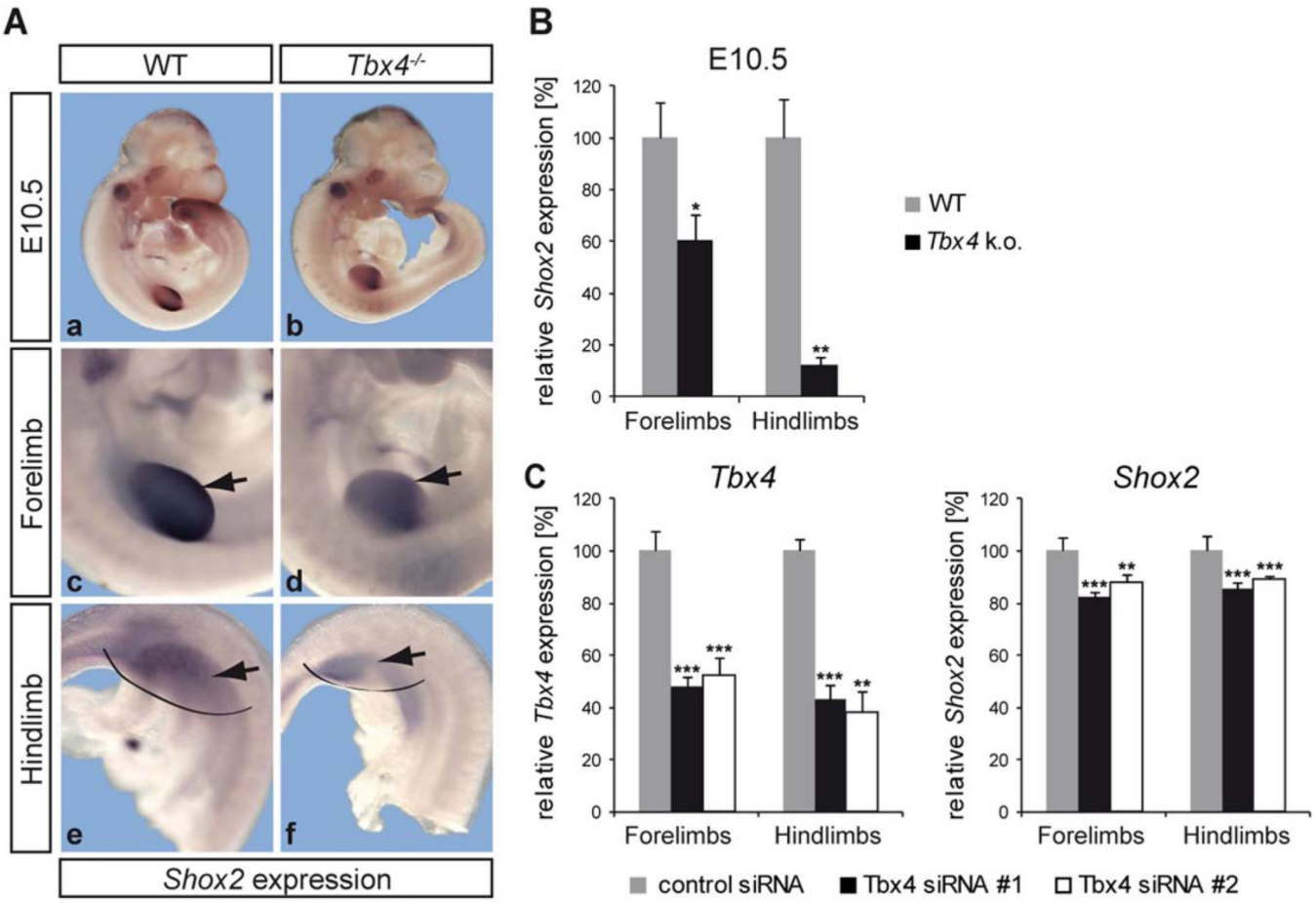

Fig. 4.

Shox2 is downregulated in *Tbx4*$^{-/-}$ fore- and hindlimbs. **A:** Whole mount in situ hybridization on E10.5 WT and *Tbx4*$^{-/-}$ embryos using a *Shox2* RNA probe shows a decreased *Shox2* expression in both fore- (d) and hindlimbs (f) of *Tbx4*$^{-/-}$ embryos (indicated by arrows). N = 7; limbs in **a, b** are magnified in **c–f. B:** Results were confirmed by qRT-PCR using WT and *Tbx4*$^{-/-}$ limb tissue. *Tbx4* knockout leads to a ∼40% decrease of *Shox2* mRNA in forelimbs and a ∼85% decrease in hindlimbs; **P* <0.05, ***P* <0.01; n = 3 independent experiments performed with 2–3 pooled embryos of 2 litters; grey bars indicate relative *Shox2* mRNA levels in WT, black bars relative *Shox2* levels in *Tbx4*$^{-/-}$**C:***Tbx4* knockdown in primary fore- and hindlimb cells. Transfection with 2 different *Tbx4* siRNAs (#1, #2), in parallel with a control siRNA, results in a ∼50–60% reduction of *Tbx4* mRNA levels after 24 hr (left), leading to a ∼10–20% downregulation of *Shox2* (right) in fore- and hindlimb cells; ***P* ≤ 0.01, ****P* ≤ 0.001; n = 10 for siRNA #1, n = 7 for siRNA #2; grey bars show relative *Tbx4/Shox2* mRNA levels after control siRNA transfection; black and white bars relative *Tbx4/Shox2* mRNA levels after *Tbx4* siRNA transfection.

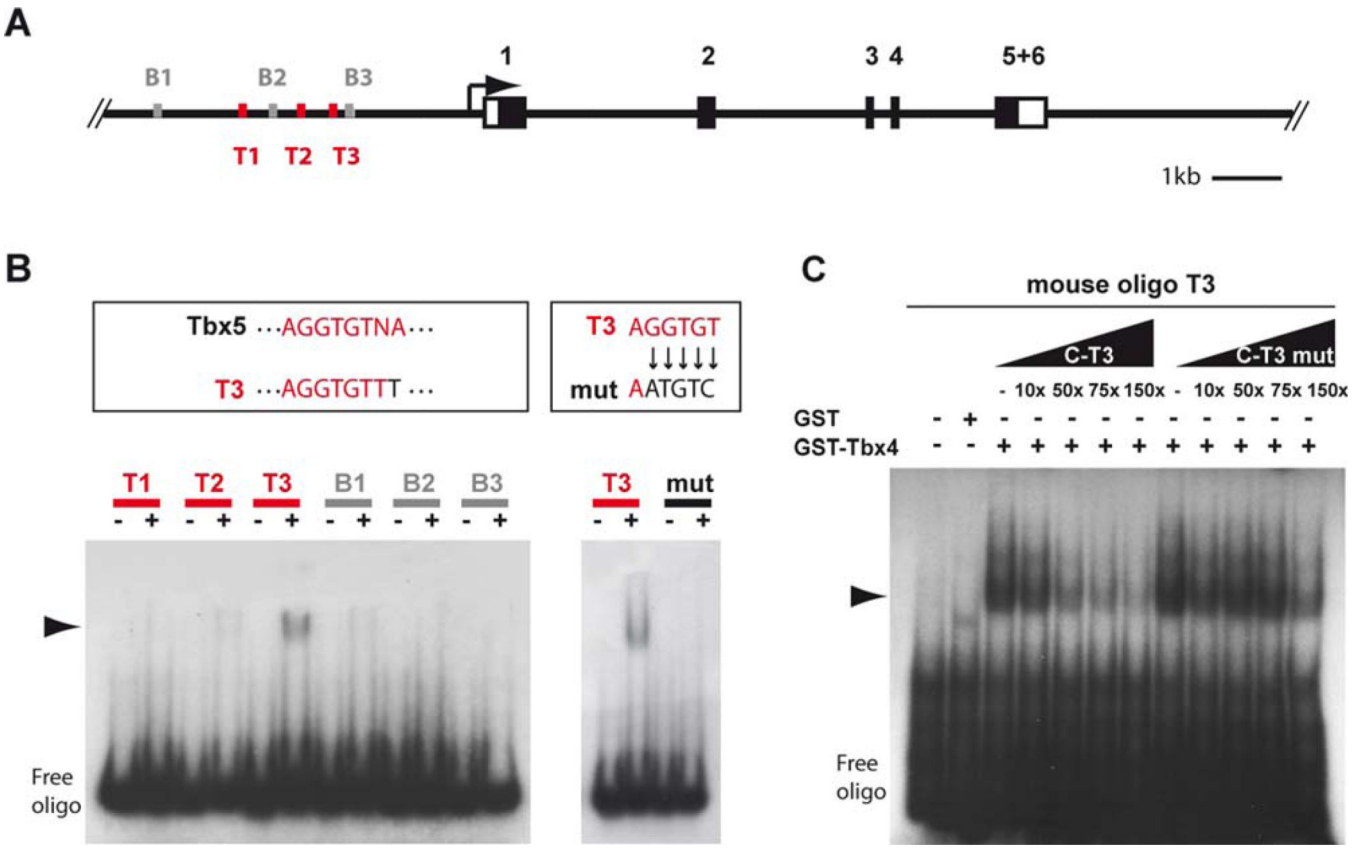

Fig. 5.

2Tbx4 binds the murine *Shox2* promoter. **A:** Schematic illustration of the murine *Shox2* gene (black boxes represent coding exons, white boxes UTRs) harbouring 3 binding sites similar to Tbx5 sites (T1–T3, red) and 3 Brachyury binding sites (B1–B3, grey) upstream of the transcriptional start site. **B:** EMSA shows specific binding of GST-Tbx4 fusion protein to an oligonucleotide containing T3 but not to T1, T2, and B1–B3 containing oligos. T3 differs from the known Tbx5 site in 1 nucleotide. Mutation of 5 nucleotides within the Tbx5 related core sequence of T3 inhibits binding of GST-Tbx4. Shift is marked by an arrowhead. **C:** Competition EMSA shows that excess (10-, 50-, 75-, and 150-fold molar) of unlabelled T3 (C-T3) decreases binding of GST-Tbx4 to labelled T3, whereas excess of mutated T3 (C-T3 mut) has no effect. Shift is marked by an arrowhead.

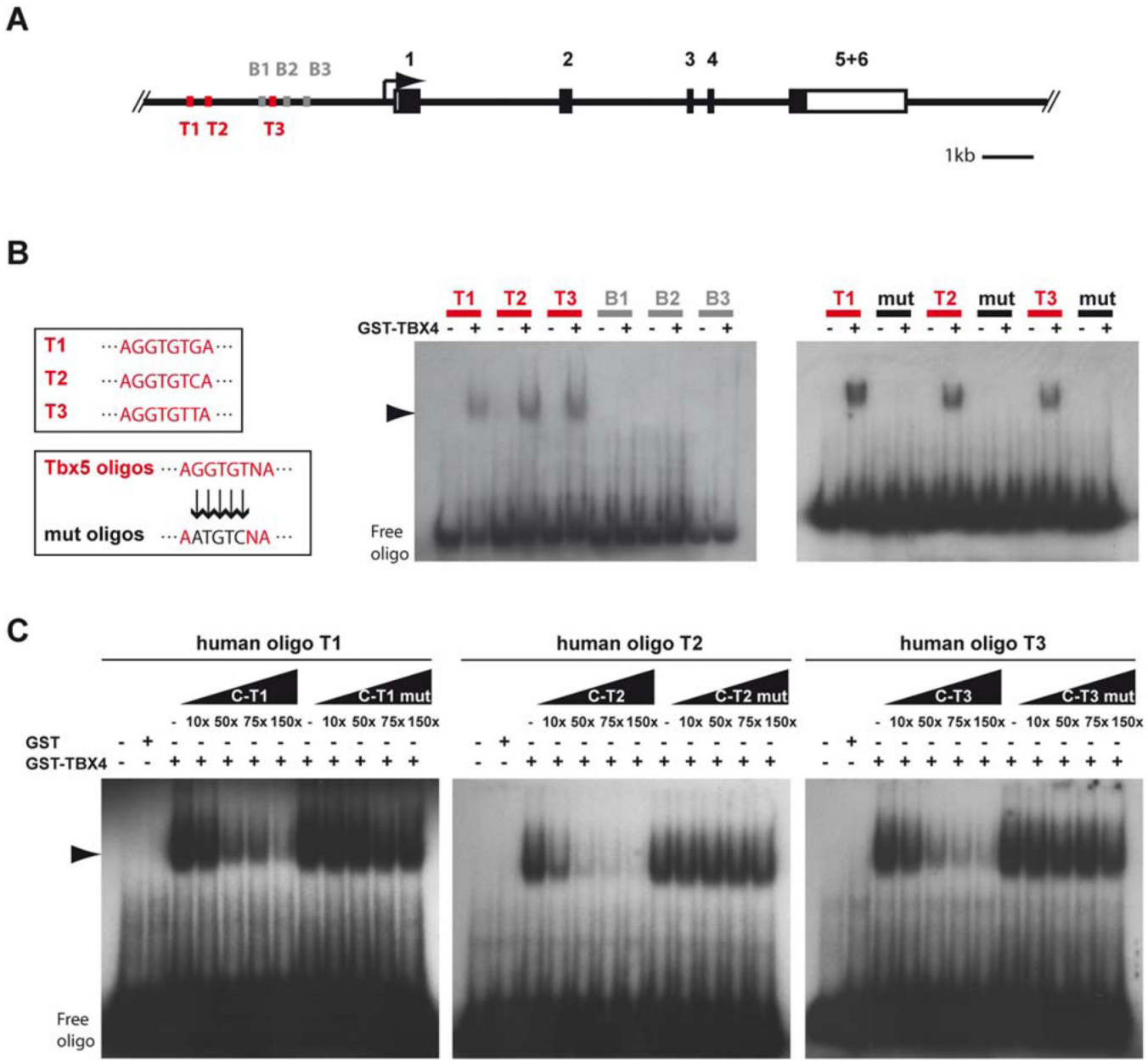

Fig. 6.

TBX4 binds the human *SH0×2* promoter. **A:** Schematic illustration of the human *SHOX2* gene (black boxes represent coding exons, white boxes UTRs) harbouring 3 TBX5 (T1–T3, red) and 3 BRACHYURY (B1-B3, grey) binding sites upstream of the transcriptional start site. **B:** EMSA shows specific binding of GST-TBX4 fusion protein to oligonucleotides containing T1–T3 but not to B1–B3 binding sites. Mutation of 5 nucleotides within the TBX5 core sequence of T1, T2, and T3 inhibits the binding of GST-TBX4. Shift is marked by an arrowhead. **C:** Competition EMSA shows that excess (10-, 50-, 75-, and 150-fold molar) of unlabelled T1 (C-T1), T2 (C-T2), and T3 (C-T3) decreases binding of GST-TBX4

to labelled T1, T2, and T3, whereas excess of mutated T1 (C-T1 mut), T2 (C-T2 mut), and T3 (C-T3 mut) has no effect. Shift is marked by an arrowhead.

TABLE 1

Oligonucleotides

Name		Sequence (5'-3')	Application
mHprt1 qRT for		TCCTCCTCAGACCGCTTTT	qRT-PCR
mHprt1 qRT rev		CCTGGTTCATCATCGCTAATC	
mSdha qRT for		CATGCCAGGGAAGATTACAAA	
mSdha qRT rev		GTTCCCCAAACGGCTTCT	
mShox2 qRT for		ACCAATTTTACCCTGGAACAAC	
mShox2 qRT rev		TCGATTTTGAAACCAAACCTG	
mTbx4 qRT for		GCATGAGAAGGAGCTGTGG	
mTbx4 qRT rev		TTACCTTGTAGCTGGGGAACA	
mTbx4 ISH for2		CCGACGAGAACAATGCTTTT	ISH probe cloning
mTbx4 ISH rev2		GCCCCGAACTCGAGTACATA	
mCol2a1 ISH for		GCCAAGACCTGAAACTCTGC	
mCol2a1 ISH rev		TTCGCAATGGATTGTGTTGT	
mSox9 ISH for		CTGAAGGGCTACGACTGGAC	
mSox9 ISH rev		CATTGACGTCGAAGGTCTCA	
mTbx4 pET41a+ BamHI for		CGCGGGATCCATGCTGCAGGATAAGGGCCTGTC	pET41a+ - *mTbx4* cloning
mTbx4 pET41a+ HindIII rev		CGCGAAGCTTGTCCATCGGTCCAGTTCTCCA	
hTBX4 pET41a+ HindIII for		TGGAGAACTGGACTGACGGACAGTCGACCGCG	pET41a+ - *hTBX4* cloning
hTBX4 pET41a+ Xhol rev		TGGAGAACTGGACTGACGGACTCGAGCGCG	
mTbx51ike_EMSA_for1	T1	GGGAAATTGGTTAGTTCCTGTTGAGCGAGGTGGAAATTCGCCCAACAATAATAAATCATGGGA	
mTbx51ike_EMSA_rev1		GGGTCCCATGATTTATTATTGTTGGGCGAATTTCCACCTCGCTCAACAGGAACTAACCAATTT	
mTbx51ike_EMSA_for2	T2	GGGGGGATATAAGAGGCTAACAGAAGAGGTGTATGTTTCCATATGTGAAAAGTTCATAAAGAA	
mTbx51ike_EMSA_rev2		GGGTTCTTTATGAACTTTTCACATATGGAAACATACACCTCTTCTGTTAGCCTCTTATATCCC	
mTbx51ike_EMSA_for3	T3	GGGACCAGGCTTCTAGCAGGGGCTATTTGGGAGGTGTTTACGAATATGTATTTCGTCATAGAG	
mTbx51ike_EMSA_rev3		GGGCTCTATGACGAAATACATATTCGTAAACACCTCCCAAATAGCCCCTGCTAGAAGCCTGGT	
Mut_mTbx51ike_EMSA_for3	T3-mut	GGGACCAGGCTTCTAGCAGGGGCTATTTGGGAATGTCTTTACGAATATGTATTTCGTCATAGAG	
Mut_mTbx51ike_EMSA_rev3		GGGCTCTATGACGAAATACATATTCGTAAAGACATTCCCAAATAGCCCCTGCTAGAAGCCTGGT	
mBrachy_EMSA_for1	B1	GGGTACGTAGCTACTTCACTGGGAGCTTTTACATCTAAGTTCAAAGATGACAACTCGAATACC	
mBrachy_EMSA_rev1		GGGGGTATTCGAGTTGTCATCTTTGAACTTAGATGTAAAAGCTCCCAGTGAAGTAGCTACGTA	
mBrachy_EMSA_for2	B2	GGGCTAGATACTAAGGTTCAGATTTCCACAGAGATTTGAGATGGAACTCACTTCCAGTATAGG	
mBrachy_EMSA_rev2		GGGCCTATACTGGAAGTGAGTTCCATCTCAAATCTCTGTGGAAATCTGAACCTTAGTATCTAG	
mBrachy_EMSA_for3	B3	GGGAAAGCAAGAGTTCATGTACTTCAATAATACCTAAATGTTTAATGCAATCGCTGTTAACCA	
mBrachy_EMSA_rev3		GGGTGGTTAACAGCGATTGCATTAAACATTTAGGTATTATTGAAGTACATGAACTCTTGCTTT	
TBX5_EMSA_for1	T1	GGGGCATCACCTGGGTCCAGACCTTTGGGCTCACACCTCCCGTTGACGTGCAAGCGCCGCAGTCC	
TBX5_EMSA_rev1		GGGGGACTGCGGCGCTTGCACGTCAACGGGAGGTGTGAGCCCAAAGGTCTGGACCCAGGTGATGC	
TBX5_EMSA_for2	T2	GGGAATCTGCATCGTAGGAAGTTTTGTTTATGACACCTACCCGAAACAAAATTGGTTATCTCACG	
TBX5_EMSA_rev2		GGGCGTGAGATAACCAATTTTGTTTCGGGTAGGTGTCATAAACAAAACTTCCTACGATGCAGATT	
TBX5_EMSA_for3	T3	GGGTTTTTGAGTTATTTGTGAATATGTATTTAACACCTCAGTTTGAGAGCACCTTGAGCACCGTA	
TBX5_EMSA_rev3		GGGTACGGTGCTCAAGGTGCTCTCAAACTGAGGTGTTAAATACATATTCACAAATAACTCAAAAA	
Mut_TBX5_EMSA_for1	T1-mut	GGGGCATCACCTGGGTCCAGACCTTTGGGCTCGACATTCCCGTTGACGTGCAAGCGCCGCAGTCC	

Name		Sequence (5’-3’)	Application
Mut_TBX5_EMSA_rev1		GGGGGACTGCGGCGCTTGCACGTCAACGGGAATGTCGAGCCCAAAGGTCTGGACCCAGGTGATGC	
Mut_TBX5_EMSA_for2	T2-mut	GGGAATCTGCATCGTAGGAAGTTTTGTTTATGGACATTACCCGAAACAAAATTGGTTATCTCACG	
Mut_TBX5_EMSA_rev2		GGGCGTGAGATAACCAATTTTGTTTCGGGTAATGTCCATAAACAAAACTTCCTACGATGCAGATT	
Mut_TBX5_EMSA_for3	T3-mut	GGGTTTTTGAGTTATTTGTGAATATGTATTTAGACATTCAGTTTGAGAGCACCTTGAGCACCGTA	
Mut_TBX5_EMSA_rev3		GGGTACGGTGCTCAAGGTGCTCTCAAACTGAATGTCTAAATACATATTCACAAATAACTCAAAAA	
BRACHY_EMSA_for1	B1	GGGAAGCTCAGTAGATGAAATATGACTTCAAACCTAAAAGTCATGTACTTAAAAAGGCAAACAA	
BRACHY_EMSA_rev1		GGGTTGTTTGCCTTTTTAAGTACATGACTTTTAGGTTTGAAGTCATATTTCATCTACTGAGCTT	
BRACHY_EMSA_for2	B2	GGGAAAGCAAGTACTGATAACAATGTATTCATACCTAAAAGCTATAGCTGCGGAAAAATTATAGA	
BRACHY_EMSA_rev2		GGGTCTATAATTTTTCCGCAGCTATAGCTTTTAGGTATGAATACATTGTTATCAGTACTTGCTTT	
BRACHY_EMSA_for3	B3	GGGGCCACACTTAGAGGTATATTTGTTTACACACTTAAATATAAC ATCATATGTAAATATTCTTT	
BRACHY_EMSA_rev3		GGGAAAGAATATTTACATATGATGTTATATTTAAGTGTGTAAACAAATATACCTCTAAGTGTGGC	